

Research Signpost
37/661 (2), Fort P.O., Trivandrum-695 023, Kerala, India



Recent Res. Dev. Optics, 3(2003): 297-318 ISBN: 81-271-0028-5

17

Review of light scattering by fiber particles with a high aspect ratio

Elena Eremina and Thomas Wriedt
Institut für Werkstofftechnik, Badgasteiner Str. 3, 28359 Bremen, Germany

Abstract

Investigation of light scattering by fibrous particles is commonly needed in particle characterization, investigation of scattering and absorption properties of interstellar dust and ice crystals and other fields. In this paper an overview of methods applied to solving this problem is presented and some numerical results obtained using these methods will be given. Because of recent progress with various methods related to the Generalized Multipole technique we will mainly focus on this methods.

1. Introduction

Light scattering computations by finite cylindrical particles having a high aspect ratio are needed in various fields e.g. Astrophysics, Atmospheric Science and Optical Particle Characterization.

In atmospheric science great attention in recent years is concentrated on ice crystals. The crystals are often in the shape of plates or needles. Mostly such interest is due to the development of satellite

communications. Satellite-communication systems operating at frequencies beyond 10 GHz are one of the main subjects in the scattering effects of ice needles in the lower atmosphere. These ice needles cause depolarization of the transmitted radiation and can severely limit system performance, particularly in the case where two orthogonal polarizations are used as separate communication channels. Extinction and absorption efficiency of ice crystals are also required for studying cloud effects on the global climate [1], [2].

Another important application is investigation of optical properties of cosmic dust grains which are detected in various astronomical objects [3], [4].

In optical particle characterization such computations are needed to design instruments to measure the size of airborne fibrous particle such as mineral, glass or asbestos fibres. Nowadays such particles are widely used, especially as insulating materials in buildings and other high temperature applications. Owing to corrosion these fibers may become airborne. Other sources of airborne fibers include natural sources (volcanic eruptions, forest fires, weathering of stones, etc.), iron smelting and combustion of coal (in coal-fired power plants, domestic stoves, etc.). Airborne fibers are considered to cause serious health hazards, depending on their material and geometric properties [5]. According to the World Health Organization (WHO), fibers are classified as hazardous, if they have length of more than $5\ \mu\text{m}$ and diameters of less than $3\ \mu\text{m}$ with length to diameter aspect ratio of more than 3:1. In this case fibers are considered respirable and may cause serious lung diseases such as cancer.

The standard procedure for the detection of respirable fibers is based on collecting of airborne fibers on a filter and classifying them under a scanning electron microscope with the human eye. This procedure is, of course, laborious and expensive as trained personnel have to detect the fibers and differentiate between the harmful and harmless ones, making it a very time-consuming method. Accuracy is another problem, as found by Höfert et al.[6]. Sending one fiber probe to different laboratories for estimation of fiber concentration led to very different results, and even the reference estimations done by four laboratories showed differences in fiber concentration of up to 40%. As this method is quite laborious, there is much interest to develop an optical online method for fiber characterization [7].

To develop such an instrument, light scattering computations are needed. For this different light scattering methods are applied. The most attractive feature of such instruments is delivering fiber geometries in a short time. In such approaches airborne fibers are illuminated by a laser beam while the scattered field is recorded with some kind of optical detector. But the most important subject is the problem of interpretation of scattering result. Only detailed investigation of measured scattering diagrams can give information about length and diameter of measured fibers. That is why during last years many computational models have been developed to study light scattering by fibrous particles. Modern methods allows to define sizes of particles their complex refractive index and aspect ratios. Usually for investigation of such particles axial symmetric models are applied.

Usually mathematical methods use the shape of a prolate spheroid or a finite cylinder as a model of a fiber. Recently many methods have been adapted for solving the light scattering problem by elongated particles. But the main problem is the sizes and aspect ratios which can be achieved. Many methods can only deal with aspect ratios up

to 5 and with length up to $1\mu\text{m}$. But real fibrous particles often have axis ratios of more than 10 and length of more than $5\mu\text{m}$. In present paper we would like to compare modern mathematical methods which are applied to solve this problem and represent some numerical results which were obtained via some of these methods.

In presented paper we will first shortly explain the methods used to compute scattering by long fibrous particle and then present some scattering diagrams as example of simulation results.

2. T-matrix method

The **T**-matrix method has been widely recognized as a powerful theoretical tool for accurately computing light scattering by optical objects. The theoretical base of **T**-matrix method was elaborated by Waterman in a series of papers [8]-[10]. Since that time many improvements of the original method have been made. Recently the original algorithm was applied to a computing of light scattering from elongated particles with aspect ratio till 4 by Mishchenko [11].

The mathematical statement of a light scattering problem in frame of **T**-matrix method consists in Maxwell's equations and boundary conditions. The fact that in the far-field zone the scattered field may be represented as spherical wave is essentially used. The scattered field connected with an incident field via scattering matrix which linearly transforms the electric vector components of the incident wave to the electric vector components of the scattered wave. The amplitude of scattering matrix depends on the directions of incidence and scattering as well as on the size, morphology, and composition of the scattering particle and on its orientation with respect to the reference frame.

Owing to the linearity of Maxwell's equations and boundary conditions, the relation between the scattered field coefficients on the one hand and the incident field coefficients on the other hand is linear and is given by a transition matrix (**T** matrix). If the **T** matrix for a given scatterer is known the scattered field can easily be computed.

A fundamental feature of the **T**-matrix approach is that the elements of the **T** matrix are independent of the incident and scattered fields and depend only on the shape, size parameter, and refractive index of the scattering particle as well as on its orientation with respect to the coordinate system. Consequently, the **T** matrix needs to be computed only once and then can be used in computations for any direction of light incidence and scattering. Another attractive feature of the method is analyticity of its mathematical formulation. Mathematical properties of all special functions used are well known and can be used to derive general properties of the **T** matrix and to analytically average light-scattering properties over particle orientations. The latter feature is of particular significance since, in most natural circumstances, particles are distributed over a range of orientations rather than being perfectly aligned.

The strategy to develop a **T**-matrix implementation for randomly oriented non-axisymmetric particles of large size parameters is based on simplification of the **T**-matrix formulation as much as possible and on using the quad precision and powerful computers [12]. Today **T**-matrix method is widely used for different kind of oblate and prolate obstacles [13]-[15]. Still, the computation investigations show that simulation of scattering by the **T**-matrix method is possible for particles with an aspect ratio till 20, this is shown for particle ($n=1.311$) of size parameter up to 12 in [16].

3. Generalized Multipole Technique (GMT)

Generalized Multipole Technique (GMT) is the name for a number of relatively new and fast advancing methods. The state of the art of the GMT is reviewed in an edited volume [17] published recently some years ago [17]. In T-matrix method the fields inside and outside a scatterer are expanded by a set of spherical multipoles having their origin at the centre of the sphere. With GMT methods many origins are applied for multipole expansion. The coefficients of this expansions are the unknown values to be determined from the boundary conditions on the particle surface. Not only multiple spherical multipoles can be used for field expansion, but also other types of sources, as long as they are solutions of the wave equation. Although the GMT methods have a history of over 35 years its popularity only increased in recent years because they were successfully extended to the analysis of a variety of wave interaction problems in piecewise linear, homogeneous, and isotropic media. Among those group of methods there is a method also named GMT, which was elaborated by Ludwig, who has considered the relatively simple case of smooth, 3-D perfectly conducting objects [18]. Since that method was expanded and applied to the analysis of light scattering by elongated obstacles by Al-Rizzo [19].

This method involves the introduction of multiple spherical multipole expansions, involving spherical Hankel functions of the first kind, with their origins located along the symmetry axis of the object for the representation of the scattered field in the exterior region. The unique feature of the proposed formulation is that the induced electric- and magnetic-field vectors in the interior scattering volume are also modeled for cases that involve spherical Bessel functions of the first kind, because the origins of the interior expansions are also located along the axis of rotational symmetry. When the incident-field vector is decomposed into azimuthal Fourier-series modes, the boundary conditions for the appropriate field components are then enforced mode by mode in the least-squares-error sense at a finite number of points across the boundaries of the domain of interest. It means that the original problem of scattering by a 3-D object can be effectively reduced to a series of two-dimensional problems. The approach suggested by Al-Rizzo [19] permits the partial decoupling of the azimuthal modal index from the system of boundary conditions relations, due to the particular choice for the origin's location of multipoles. The maximal aspect ratio achieved by that approach is 10 for spheroidal particle with $\epsilon = 2.25$, $kl = 10$ (ϵ is permittivity, l is particle length, k is a wave vector) under wavelength $\lambda = 10\mu m$ [19].

3.1 Multiple Multipole Method (MMP)

The Multiple Multipole Method (MMP) is another variant from different powerful numerical methods on base of GMT. MMP was developed by Hafner and Bomholt [20] for general electromagnetic computations. It also was modified for cylinders [21]. In recent time in frame of this approach a bent fiber was calculated [22]. It is a semi-analytical method, in the sense that the electromagnetic fields are expressed as a linear combination of multiple multipoles, while the amplitudes of the multipoles are obtained by enforcing the boundary conditions in a set of matching points.

The mathematical statement of light scattering problem in frame of MMP consists in system of Maxwell's equations, transmission condition at a particle surface and

condition at infinity to provide the unique solution. We will consider scattering in an isotropic homogeneous medium in R^3 of an electromagnetic wave from a local homogeneous penetrable obstacle D_i with the smooth boundary S and exterior domain D_s . The scattered electromagnetic field $\mathbf{E}_s, \mathbf{H}_s \in D_s$ and the internal electromagnetic fields $\mathbf{E}_i, \mathbf{H}_i \in D_i$ satisfying the Maxwell equations

$$\begin{aligned} \nabla \times \mathbf{E}_t - jk_t \mu_t \mathbf{H}_t &= 0 \\ \nabla \times \mathbf{H}_t - jk_t \epsilon_t \mathbf{E}_t &= 0 \end{aligned} \quad t = i, s \quad (1)$$

and the boundary condition at the particle boundary

$$\begin{aligned} \mathbf{n} \times \mathbf{E}_i - \mathbf{n} \times \mathbf{E}_s - \mathbf{n} \times \mathbf{E}_0 &= 0 \\ \mathbf{n} \times \mathbf{H}_i - \mathbf{n} \times \mathbf{H}_s - \mathbf{n} \times \mathbf{H}_0 &= 0 \end{aligned} \quad (2)$$

The scattered field $\mathbf{E}_s, \mathbf{H}_s$ additionally fulfill the Silver Müller radiation condition at infinity:

$$\lim_{r \rightarrow \infty} \left(\sqrt{\epsilon_s} \mathbf{E}_s \times \frac{\mathbf{r}}{r} - \sqrt{\mu_s} \mathbf{H}_s \right) = 0, \quad r = |M| \rightarrow \infty. \quad (3)$$

Here $\{\mathbf{E}^0, \mathbf{H}^0\}$ is an exciting field, \mathbf{n} is the unit outward normal to S , \times is a sign of vector product, index s belongs to the external domain D_s and i to domain inside the particle D_i , μ_t and ϵ_t are the permeability and the permittivity of domain D_t respectively.

An approximate solution $\mathbf{E}_i^N, \mathbf{H}_i^N$ of the scattering problem is constructed as a finite linear combination of fields of multiple multipoles having different origins. For the scattered field these multipoles will be located inside D_s , so that $\mathbf{E}_s^N, \mathbf{H}_s^N$ is a radiating solution to the Maxwell equations being regular in D_s . For the internal field $\mathbf{E}_i^N, \mathbf{H}_i^N$ the radiating multipoles are distributed in D_s , while the regular ones are located inside D_i . The origins of the multipoles are distributed according to the shape of the domain. It can be shown [23], that the following estimate holds for the approximate solution:

$$\begin{aligned} & \|\mathbf{E}_s - \mathbf{E}_s^N\|_{\infty, G_s} + \|\mathbf{H}_s - \mathbf{H}_s^N\|_{\infty, G_s} + \|\mathbf{E}_i - \mathbf{E}_i^N\|_{\infty, G_i} + \|\mathbf{H}_i - \mathbf{H}_i^N\|_{\infty, G_i} \\ & \leq C (\|\mathbf{n} \times \mathbf{E}_s^N + \mathbf{n} \times \mathbf{E}_0 - \mathbf{n} \times \mathbf{E}_i^N\|_{2, S} + \|\mathbf{n} \times \mathbf{H}_s^N + \mathbf{n} \times \mathbf{H}_0 - \mathbf{n} \times \mathbf{H}_i^N\|_{2, S}) \end{aligned} \quad (4)$$

with $G_s \subset D_s$ and $G_i \subset D_i$

C is a constant depending on G_s and S .

According to the above estimate a quasisolution to the boundary value condition can be obtained by approximating the tangential components of the incident fields $\mathbf{E}_0, \mathbf{H}_0$ on the boundary of the scatterer by multiple multipoles. For estimate (4) to be valid the

system of multiple multipoles is required to be complete which has been proven by Doicu [24].

The implementation of MMP into a numerical algorithm for calculation of the fields of a dielectric scatterer is done the following way.

$$\begin{aligned}\mathcal{M}_{mnp}^3 &= \mathbf{M}_{mn}^3 [k_t (\mathbf{x} - \mathbf{x}_{0p})] \\ \mathcal{N}_{mnp}^3 &= \mathbf{N}_{mn}^3 [k_t (\mathbf{x} - \mathbf{x}_{0p})]\end{aligned}\quad (5)$$

are radiating spherical vector wave functions solving the Maxwell equations with \mathbf{x}_{0p} as the position of the pole p and $\{\mathbf{n} \times \mathcal{M}_{mnp}^3, \mathbf{n} \times \mathcal{N}_{mnp}^3\}$ are linearly independent and complete. \mathbf{M}_{mn}^3 and \mathbf{N}_{mn}^3 are defined as

$$\begin{aligned}\mathbf{M}_{mn}^3 &= h_n(kr) \left[jm \frac{P_n^{|m|}(\cos \theta)}{\sin \theta} \mathbf{e}_\theta - \frac{dP_n^{|m|}(\cos \theta)}{d\theta} \mathbf{e}_\varphi \right] e^{jm\varphi} \\ \mathbf{N}_{mn}^3 &= \left\{ \begin{array}{l} n(n+1) \frac{h_n(kr)}{kr} P_n^{|m|}(\cos \theta) \mathbf{e}_r \\ + \frac{[kr h_n(kr)]'}{kr} \left[\frac{dP_n^{|m|}(\cos \theta)}{d\theta} \mathbf{e}_\theta + jm \frac{P_n^{|m|}(\cos \theta)}{\sin \theta} \mathbf{e}_\varphi \right] \end{array} \right\} e^{jm\varphi}\end{aligned}\quad (6)$$

where $(\mathbf{e}_r, \mathbf{e}_\varphi, \mathbf{e}_\theta)$ are the unit vectors in spherical coordinates, n is the order of the multipole, m is the azimuthal mode, h_n denotes the Hankel function and $P_n^{|m|}$ are the Legendre polynomials.

The approximated internal and scattered electric fields \mathbf{E}_i^N are represented as linear combination of radiating functions

$$\mathbf{E}_s^N = \sum_{p=1}^P \sum_{n=1}^{N_p} \sum_{m=-n}^n a_{mnp}^{N_p} \mathcal{M}_{mnp}^{3s} + b_{mnp}^{N_p} \mathcal{N}_{mnp}^{3s}\quad (7)$$

$$\mathbf{E}_i^N = \sum_{p=1}^P \sum_{n=1}^{N_p} \sum_{m=-n}^n c_{mnp}^{N_p} \mathcal{M}_{mnp}^{3i} + d_{mnp}^{N_p} \mathcal{N}_{mnp}^{3i}\quad (8)$$

The expansion coefficients $a_\mu^N, b_\mu^N, c_\mu^N$ and d_μ^N may be solved by minimizing the residual field:

$$\mathbf{a} = \arg \min \left\{ \|\mathbf{n} \times \mathbf{E}_s^N + \mathbf{n} \times \mathbf{E}_0 - \mathbf{n} \times \mathbf{E}_i^N\|_{2,S}^2 + \|\mathbf{n} \times \mathbf{H}_s^N + \mathbf{n} \times \mathbf{H}_0 - \mathbf{n} \times \mathbf{H}_i^N\|_{2,S}^2 \right\},\quad (9)$$

$$\text{with } \mathbf{a} = \begin{bmatrix} a_\mu^N \\ b_\mu^N \\ c_\mu^N \\ d_\mu^N \end{bmatrix}$$

While the approximate solution $\mathbf{E}_i^N, \mathbf{H}_i^N$ converges to the exact solution $\mathbf{E}_i, \mathbf{H}_i$ the relative error may be evaluated by

$$\varepsilon_N = \frac{\|\mathbf{n} \times \mathbf{E}_s^N + \mathbf{n} \times \mathbf{E}_0 - \mathbf{n} \times \mathbf{E}_i^N\|_{2,S} + \|\mathbf{n} \times \mathbf{H}_s^N + \mathbf{n} \times \mathbf{H}_0 - \mathbf{n} \times \mathbf{H}_i^N\|_{2,S}}{\|\mathbf{n} \times \mathbf{E}_0\|_{2,S} + \|\mathbf{n} \times \mathbf{H}_0\|_{2,S}} \quad (10)$$

In order to reduce the computational effort the surface of the scatterer has to be discretized. Thus the surface is divided into J cells, so called matching points, with the coordinate $y_j, j = 1 \dots J$ being in the center of each cell. The expansion coefficients can then be calculated by a least square problem:

$$\mathbf{a} = \arg \min \|\mathbf{A}\mathbf{x} - \mathbf{f}\|_2^2 \quad (11)$$

where the matrix \mathbf{A} and the vector \mathbf{f} depend on the values of the basis functions $\{\Psi_\mu^{3s}, \Phi_\mu^{3s}, \Psi_\mu^{3i}, \Phi_\mu^{3i}\}$ and the incident field at the matching points, respectively. \mathbf{A} is rectangular matrix with the number of matching points J being larger than the number of multipoles. Equation (11) is solved by using QR decomposition, which is done with an algorithm based on Givens rotations.

The convergence and stability of the solutions is very sensitive to the following rules:

The density of matching points has to be chosen so that the distance of adjacent matching points is much less than the wavelength of the incident beam.

The multipoles do not have to be placed too far off or too close to the surface of the scatterer, otherwise a well-conditioned rectangular matrix will not be constructed.

Because of its local behavior, each multipole influences only a restricted area on the surface of the scattering body. Thus multipoles have to be distributed to have the whole surface of the scatterer covered by the area of influence of at least one multipole.

The maximum order of each multipole is also restricted to avoid an oscillatory solution.

Because the origin of multipoles can be set very flexible, MMP is able to calculate the field of arbitrary shaped objects, especially cylinders with a large aspect ratio and bent fibers [22].

3.2 Discrete Sources Method (DSM)

Another well known variant of GMT which is a recently applied to long fibers is Discrete Sources Method (DSM). Originally theoretical principles of DSM were established about 35 years ago by Kupradze in Soviet Union [25] and Yasuura in Japan [26]. The first version of DSM was published in 1980 [27], since that several research groups were working in this direction worldwide [17]. Recently the method was modified for light scattering from different kind objects [28], [29], and for evanescent wave scattering [30].

The mathematical statement of light scattering problem in a frame of DSM consists in system of Maxwell's equations, transmission condition at a particle surface and condition at infinity to provide an unique solution. The approximate solution is constructed as a linear combination of multipole's fields with a certain amplitudes, in such way that it satisfies the Maxwell's equations and conditions at infinity. To determine the amplitudes of the solution the condition at a particle surface is used. That allows to estimate the residual of obtained solution and reduce a time demands.

We use (z, θ, φ) - as cylindrical coordinate system. We assume the time dependence to be $\exp(j\omega t)$. Scattering is described by the electromagnetic fields $\{\mathbf{E}_t, \mathbf{H}_t\}$ satisfying the Maxwell equations

$$\begin{aligned} \nabla \times \mathbf{H}_t - jk\epsilon_t \mathbf{E}_t &= 0; \\ \nabla \times \mathbf{E}_t + jk\mu_t \mathbf{H}_t &= 0 \end{aligned} \quad \text{in } D_t, \quad t = s, i, \quad D_s := R^3 / \bar{D}_i \quad (12)$$

transmission condition enforced on the particle surface (2) and Silver-Muller conditions at infinity (3).

Here $\text{Im } \epsilon_s, \mu_s = 0, \text{Im } \epsilon_i, \mu_i \leq 0$. The boundary value scattering problem is wellknown to have an unique solution [31].

In the frame of DSM the approximate solution is constructed as a finite linear combinations of the field of dipoles and multipoles deposited in some supplementary domain. Under these conditions the representation satisfies Maxwell equations in $D_{i,s}$ and radiation conditions at infinity. The unknown amplitudes of DS are to be determined from the transmission conditions at the boundary S . So, the boundary value scattering problem under investigation is reduced to the solution of an approximation problem enforced at an obstacle surface [32].

$$\begin{aligned} \mathbf{n} \times (\mathbf{E}_i - \mathbf{E}_s) &= \mathbf{n} \times \mathbf{E}_0, \\ \mathbf{n} \times (\mathbf{H}_i - \mathbf{H}_s) &= \mathbf{n} \times \mathbf{H}_0, \end{aligned} \quad S. \quad (13)$$

One of the most attractive features of DSM consists in flexible choice of DS fields that can be used for approximate solution construction. There are no limitations to a choice of DS support, which should provide fulfilling the Maxwell equations, radiation conditions and yield a complete system of DS fields at the obstacle surface [32].

We will consider an axial symmetrical particle, then the system of lowest order multipoles distributed over the axis of symmetry can be applied to construction an approximation solution construction. As a consequence the surface approximating problem can be reduced to a number of one dimensional problems enforced at the particle generatrix.

Let the axis of symmetry be the Z -axis, DS $\{z_n\}_{n=1}^{\infty}$ distributed over a segment ω_0 of the Z -axis, situated inside a particle, which is chosen as a closed multitude with at least one condensing point. Then the follow results are valid [24]:

1. Let the DS support be ω_0 , then the associated system of electrical lowest order distributed multipoles

$$\nabla \times \nabla \times [Y_m^e(\rho, z_n^e) \{1, \cos m\varphi, \sin m\varphi\} \{\mathbf{e}_i\}], \quad \eta \in L, \quad \{z_n^e\} \in \omega_0, \quad n, m \in N. \quad (14)$$

L - generatrix of S ,

is a complete system at any closed smooth axial symmetric surface, confining ω_0 . Here $Y_m^e(\rho, z_n^e) = h_m^{(2)}(k_e R_{\eta z_n^e}) \cdot (r/R_{\eta z_n^e})^m$, where $h_m^{(2)}(\cdot)$, is spherical Hankel function, $R_{\eta z_n^e} = r^2 + (z - z_n^e)^2$, z_n^e are multipoles coordinates inside a particle, $\{\mathbf{e}_i\} = \{e_x, e_y, e_z\}$ is a vector basis in Cartesian coordinate system.

2. The system of magnetic multipoles distributed over ω_0 is complete

$$\nabla \times [Y_m^e(\rho, z_n^e) \{1, \cos m\varphi, \sin m\varphi\} \{\mathbf{e}_i\}], \quad n, m \in N. \quad (15)$$

3. For internal fields representation similar results hold. The system of electrical lowest order regular functions is complete at ∂D_i

$$\nabla \times \nabla \times [Y_m^i(\rho, z_n) \{1, \cos m\varphi, \sin m\varphi\} \{\mathbf{e}_i\}], \quad n, m \in N. \quad (16)$$

where $Y_m^i(\rho, z_n) = j_m(k_i R_{\eta z_n}) \cdot (r/R_{\eta z_n})^m$, $j_m(\cdot)$ is spherical Bessel function.

The same result may be formulated for the system of magnetic regular functions

$$\nabla \times [Y_m^i(\rho, z_n) \{1, \cos m\varphi, \sin m\varphi\} \{\mathbf{e}_i\}]. \quad (17)$$

These systems represent systems of regular functions, which satisfy Maxwell equation in the whole space R^3 .

We will construct the approximate solution by taking into account not only the rotational symmetry of the obstacle, but also the polarization of an external excitation as well.

In case of a P-polarization exciting plane wave the field accepts the following form

$$\begin{aligned} \mathbf{E}_0 &= (\mathbf{e}_x \cos \theta_0 + \mathbf{e}_z \sin \theta_0) \gamma, \\ \mathbf{H}_0 &= -\mathbf{e}_y \gamma \cos \theta_0, \quad \gamma = \exp\{-jk_s(x \sin \theta_0 - z \cos \theta_0)\}; \end{aligned} \quad (18)$$

where $k_s = k\sqrt{\epsilon_s \mu_s}$, θ_0 -incident angle

To take the polarization of external excitation into account we use some linear combination of electrical and magnetic multipoles. For this we need special vector potentials. In case of P-polarization of the plane wave the representation for vector potentials in a cylindrical coordinate system can be represented as

$$\begin{aligned} \mathbf{A}_{mn}^{1,s,i} &= \left\{ Y_m^{s,i}(\rho, z_n^{s,i}) \cos(m+1)\phi; -Y_m^{s,i}(\rho, z_n^{s,i}) \sin(m+1)\phi; 0 \right\}, \\ \mathbf{A}_{mn}^{2,s,i} &= \left\{ Y_m^{s,i}(\rho, z_n^{s,i}) \sin(m+1)\phi; Y_m^{s,i}(\rho, z_n^{s,i}) \cos(m+1)\phi; 0 \right\} \end{aligned} \quad (19)$$

Vector potentials for vertical dipoles, which are required to be added to provide completeness of the multipoles's system are

$$\mathbf{A}_n^{3,s,i} = \left\{ 0, 0, Y_0^{s,i}(\rho, z_n^{s,i}) \right\}. \quad (20)$$

So, the approximate solution taking into account P-polarization of the plane wave, axial symmetry of the particle, can be represented in the form

$$\begin{pmatrix} \mathbf{E}_t^N \\ \mathbf{H}_t^N \end{pmatrix} = \sum_{m=0}^M \sum_{n=1}^{N_t^m} \{ p_{mn}^t D_1 \mathbf{A}_{mn}^{1,t} + q_{mn}^t D_2 \mathbf{A}_{mn}^{2,t} \} + \sum_{n=1}^{N_t^0} r_n^t D_1 \mathbf{A}_n^{1,t} \quad (21)$$

here

$$D_1 = \begin{pmatrix} \frac{j}{k\epsilon_\xi \mu_\xi} \nabla \times \nabla \times \\ -\frac{1}{\mu_\xi} \nabla \times \end{pmatrix}, \quad D_2 = \begin{pmatrix} \frac{1}{\epsilon_\xi} \nabla \times \\ \frac{j}{k\epsilon_\xi \mu_\xi} \nabla \times \nabla \times \end{pmatrix}.$$

Then the following result holds:

The approximate solution (21) converges to the exact one under $\{M, N_t^m\}$ tend to infinity.

In the case of an S-polarized plane wave the exciting field has the form:

$$\begin{aligned} \mathbf{E}_0 &= \mathbf{e}_y \gamma \cos \theta_0, \\ \mathbf{H}_0 &= (\mathbf{e}_x \cos \theta_0 + \mathbf{e}_z \sin \theta_0) \gamma. \end{aligned} \quad (22)$$

The vector potentials corresponding to this case are

$$\begin{aligned} \mathbf{A}_{mn}^{1,s,i} &= \left\{ Y_m^{s,i}(\rho, z_n^{s,i}) \sin(m+1)\phi; Y_m^{s,i}(\rho, z_n^{s,i}) \cos(m+1)\phi; 0 \right\}, \\ \mathbf{A}_{mn}^{2,s,i} &= \left\{ Y_m^{s,i}(\rho, z_n^{s,i}) \cos(m+1)\phi; -Y_m^{s,i}(\rho, z_n^{s,i}) \sin(m+1)\phi; 0 \right\}. \end{aligned} \quad (23)$$

Hence the approximate solution can be represented as

$$\begin{pmatrix} \mathbf{E}_t^N \\ \mathbf{H}_t^N \end{pmatrix} = \sum_{m=0}^M \sum_{n=1}^{N_t^m} \{ p_{mn}^t D_1 \mathbf{A}_{mn}^{1,t} + q_{mn}^t D_2 \mathbf{A}_{mn}^{2,t} \} + \sum_{n=1}^{N_t^0} r_n^t D_2 \mathbf{A}_{0n}^{1,t} \quad (24)$$

The approximate solution (24) corresponding to S-case converges to the exact one under $\{M, N_t^m\}$ tend to infinity.

Next we would like to briefly explain the numerical algorithm of the method.

Let us remind that the approximate solutions for cases of P (21) and S polarization (24) satisfy Maxwell's equation (12) and radiating conditions at infinity (3). As the DS are situated on the symmetry axis of the particle, that results the approximate solution is a finite linear combination of Fourier harmonics with respect to ϕ angle variable. So, at first we resolve the plane wave excitation in a Fourier series with respect to ϕ variable, using the following resolution for the plane wave:

$$\exp\{-jk_s\rho\sin\theta_0\cos\phi\} = \sum_{m=0}^{\infty} (2 - \delta_{0m}) (-j)^m J_m(k_s\rho\sin\theta_0) \cos m\phi, \quad (25)$$

θ_0 – the incident angle of plane wave.

The approximate solution satisfies all the conditions of original scattering problem, except the transmission conditions. Therefore, the unknown vector of amplitudes of DS

$$\mathbf{p}_m = \{p_{mn}^{s,i}, q_{mn}^{s,i}, r_n^{s,i}\}_{n=1}^{N_m^m} \quad (26)$$

where $p_{mn}^{s,i}$ are amplitudes of electric, $q_{mn}^{s,i}$ – magnetic and $r_n^{s,i}$ – vector dipoles in representations (21), (24), is to be determined from the transmission conditions (13). Taking into account the dependence of plane wave on the φ angle, we can reduce the surface approximation problem enforced at the particle surface into a sequence of one-dimensional problems at the particle generatrix L . For solving this problem we will use the General Matching-Point Technique [33]. At first we choose matching points $\{\eta_l\}_{l=1}^L$ distributed homogeneously over L . Then by matching the representation for the approximate solution and external excitation at the set of matching points and using the axial symmetry we pass from the surface approximation to the approximation for each Fourier harmonic. As a consequence the unknown vectors of amplitudes \mathbf{p}_m can be found as a pseudosolution of a over-determined system of linear equations

$$\mathbf{B}_m \mathbf{p}_m = \mathbf{q}_m, \quad m = 0, \dots, M. \quad (27)$$

here \mathbf{B}_m is a rectangular matrix, $\mathbf{B}_m [B_{il}^m], l = 1, \dots, 4L, i = 1, \dots, 2(N_i^m + N_e^m)$. The reasonable ratio of matching points and number of DS was established as $2 < L/(N_i^m + N_e^m) < 4$, the vector of unknown amplitudes \mathbf{p}_m has length $2(N_i^m + N_e^m)$ the vector in the right-hand side can be represented as a $4L$ vector, in the following form

$$\mathbf{q}_m = \left(e_{m+1,l}^{0\tau}, e_{m+1,l}^{0\varphi}, h_{m+1,l}^{0\tau}, h_{m+1,l}^{0\varphi} \right)^T \quad (28)$$

here $e_{ml}^{0\tau,\varphi} = e_{ml}^{0\tau,\varphi}(\eta_l), h_{ml}^{0\tau,\varphi} = h_{ml}^{0\tau,\varphi}(\eta_l)$. The components of the vector, in case of P polarized plane wave excitation can be written as:

$$\begin{aligned} e_{m+1}^{0\tau}(\eta) &= (-j)^m \alpha \cos\theta_0 [(J_m(k_e\rho\sin\theta_0) - J_{m+2}(k_e\rho\sin\theta_0)) + 2j\beta\sin\theta_0 J_{m+1}(k_e\rho\sin\theta_0)] \times \\ &\quad \times \exp\{-jk_e z \cos\theta_0\}, \\ e_{m+1}^{0\varphi}(\eta) &= -\cos\theta_0 (-j)^m [J_m(k_e\rho\sin\theta_0) + J_{m+2}(k_e\rho\sin\theta_0)] \exp\{-jk_e z \cos\theta_0\}, \\ h_{m+1}^{0\tau}(\eta) &= -\alpha (-j)^m [J_m(k_e\rho\sin\theta_0) + J_{m+2}(k_e\rho\sin\theta_0)] \exp\{-jk_e z \cos\theta_0\}, \\ h_{m+1}^{0\varphi}(\eta) &= (-j)^m [-J_m(k_e\rho\sin\theta_0) + J_{m+2}(k_e\rho\sin\theta_0)] \exp\{-jk_e z \cos\theta_0\}. \end{aligned} \quad (29)$$

In case of S-polarized exciting wave:

$$\begin{aligned}
e_{m+1}^{0r}(\eta) &= (-j)^m \alpha [J_m(k_e \rho \sin \theta_0) + J_{m+2}(k_e \rho \sin \theta_0)] \exp\{-jk_e z \cos \theta_0\}, \\
e_{m+1}^{0\varphi}(\eta) &= (-j)^m [J_m(k_e \rho \sin \theta_0) - J_{m+2}(k_e \rho \sin \theta_0)] \exp\{-jk_e z \cos \theta_0\}, \\
h_{m+1}^{0r}(\eta) &= (-j)^m [\alpha \cos \theta_0 (J_m(k_e \rho \sin \theta_0) - J_{m+2}(k_e \rho \sin \theta_0)) + 2j\beta \sin \theta_0 J_{m+1}(k_e \rho \sin \theta_0)] \times \\
&\quad \times \exp\{-jk_e z \cos \theta_0\}, \\
h_{m+1}^{0\varphi}(\eta) &= -\cos \theta_0 (-j)^m [J_m(k_e \rho \sin \theta_0) + J_{m+2}(k_e \rho \sin \theta_0)] \exp\{-jk_e z \cos \theta_0\},
\end{aligned} \tag{30}$$

here $(\alpha, 0, \beta)$ - vector, tangential to the generatrix at η -point, (ρ, z) correspond to the coordinates of matching point.

Because Fourier harmonics do not depend on the φ angle, corresponding to vertical electric or magnetic dipoles linear system for P and S polarization can be written in the form

$$\mathbf{B}_{-1}\mathbf{p}_{-1} = \mathbf{q}_{-1}.$$

In this case \mathbf{B}_{-1} has a dimension $2L \times (N_i^m + N_s^m)$, the right-hand side vector has length $2L$, and the unknown vector of amplitudes has length $(N_i^m + N_s^m)$. Then we have

$$\begin{aligned}
e_0^{0\varphi}(\eta) &= -[j\alpha \cos \theta_0 J_1(k_s \rho \sin \theta_0) + \beta \sin \theta_0 J_0(k_s \rho \sin \theta_0)] \exp\{-jk_s z \cos \theta_0\}, \\
h_0^{0r}(\eta) &= jJ_1(k_s \rho \sin \theta_0) \exp\{-jk_s z \cos \theta_0\},
\end{aligned} \tag{31}$$

for P polarization and for S case:

$$\begin{aligned}
e_0^{0r}(\eta) &= jJ_1(k_s \rho \sin \theta_0) \exp\{-jk_s z \cos \theta_0\}, \\
h_0^{0\varphi}(\eta) &= -[j\alpha \cos \theta_0 J_1(k_s \rho \sin \theta_0) + \beta \sin \theta_0 J_0(k_s \rho \sin \theta_0)] \exp\{-jk_s z \cos \theta_0\}.
\end{aligned} \tag{32}$$

The main differences of the extended DSM scheme described above to the conventional DSM one [17] consist in the following:

1. Different numbers of DS N_i^m , N_s^m are possible for the representation of the scattered field outside and total field inside the particle. The numbers of DS are chosen proportionally to the value of refractive index of the corresponding media. For the internal domain (higher refractive index $\sqrt{\varepsilon_i \mu_i} > \sqrt{\varepsilon_s \mu_s}$) we use a higher number of DS then for the scattered field $N_i^m > N_s^m$.
2. The number of DS depends on the rank of Fourier harmonics $N_t^m = N_t(m)$. For higher harmonics we use a lower number of multipoles $N_\xi^{m+1} \leq N_\xi^m$. This circumstance enables to acquire a more accurate simulation result, provides a monotone decrease of the surface residual and to reduce the demand on computer resources up to 30% for a larger particles compared to the conventional DSM model [32]. Besides it allows to extend the range of validity of the DSM for the particles of larger diameters.

After DS amplitudes $\{\mathbf{p}_m\}_{m=-1}^M$ have been determined can be computed the Far Field Pattern [31]:

$$\frac{\mathbf{E}(\mathbf{r})}{|\mathbf{E}^0(\mathbf{r})|} = \frac{\exp(-jk_s r)}{r} \mathbf{F}(\theta, \phi) + o\left(\frac{1}{r}\right), \quad r \rightarrow \infty. \quad (33)$$

The vector $\mathbf{F}(\theta, \phi)$ has two components in the far zone ϕ and θ , so that its components are determined at the unit sphere as

$$\mathbf{F}(\theta, \phi) = \theta \cdot F_\theta(\theta, \phi) + \phi \cdot F_\phi(\theta, \phi) \quad (34)$$

Using asymptotic representation for Y_{mn} for a P-polarized exciting plane wave the Far Field Pattern accepts the form

$$\begin{aligned} F_\theta^P(\theta, \phi) &= j \sum_{m=0}^M \cos(m+1)\phi (j \sin \theta)^m \sum_{n=1}^{N_s^m} \{p_{mn}^s \cos \theta + q_{mn}^s\} G_n - j \sin \theta \sum_{n=1}^{N_s^0} r_n^s G_n, \\ F_\phi^P(\theta, \phi) &= -j \sum_{m=0}^M \sin(m+1)\phi (j \sin \theta)^m \sum_{n=1}^{N_s^m} \{p_{mn}^s + q_{mn}^s \cos \theta\} G_n, \quad G_n = \exp\{-jz_n \cos \theta\}. \end{aligned} \quad (35)$$

Last term in F^P corresponds to vertical dipoles.

For S-polarized excitation the far field components can be written as follows:

$$\begin{aligned} F_\theta^S(\theta, \phi) &= j \sum_{m=0}^M \sin(m+1)\phi (j \sin \theta)^m \sum_{n=1}^{N_s^m} \{p_{mn}^s \cos \theta - q_{mn}^s\} G_n, \\ F_\phi^S(\theta, \phi) &= j \sum_{m=0}^M \cos(m+1)\phi (j \sin \theta)^m \sum_{n=1}^{N_s^m} \{p_{mn}^s - q_{mn}^s \cos \theta\} G_n + j \sin \theta \sum_{n=1}^{N_s^0} r_n^h G_n, \end{aligned} \quad (36)$$

In last investigations in fiber sizing using DSM the aspect ratio of 100 was achieved for cylinder of length=30 μ m, under $\lambda=0.488 \mu$ m [34].

3.3 Null-field method with discrete sources

The Null-field method with discrete sources is a another formal modification of a classical GMT method, discussed in [24]. Essentially, in this method different types of discrete sources are used for approximating the surface current densities on the surface of the scattering particle. The discrete sources are placed on a certain support in an additional region with respect to the region where the solution is required [35]. Unknown amplitudes of discrete sources which produce the surface current densities are computed by using the null-field condition for the total electric field on the particle surface.

Recently this method was applied to the electromagnetic scattering from scatterers with complex structure [36].

As a full theoretical outline of the null-field method with discrete sources has been given in [24], this paper we will only give a brief description of the theory.

We denote the domain contained inside the cylinder with D_i and the space outside with D_s . The fiber surface is denoted by S . Given \mathbf{E}_0 and \mathbf{H}_0 as complete solution to the

Maxwell equations representing an incident electromagnetic field, we should find the vector fields $\mathbf{E}_s, \mathbf{H}_s$ in the free space and $\mathbf{E}_i, \mathbf{H}_i$ inside the scatterer, satisfying the reduced Maxwell equations:

$$\begin{aligned} \nabla \times \mathbf{E}_t - jk_t \mathbf{H}_t &= 0 \\ \nabla \times \mathbf{H}_t + jk_t \mathbf{E}_t &= 0 \end{aligned} \quad \text{in } D_t, t = s, i. \quad (37)$$

and the transmission conditions on the particle boundary (2).

In addition, the scattered fields \mathbf{E}_s and \mathbf{H}_s must satisfy the Silver-Müller radiation condition (3).

For solving the transmission boundary-value problem in the framework of the null-field method with discrete sources, the scattering object is replaced by a set of surface current densities \mathbf{e} and \mathbf{h} , so that in the exterior region the sources and the fields are exactly the same as those existing in the original scattering problem.

A set of integral equations for the surface current densities \mathbf{e} and \mathbf{h} is derived for a set of distributed lowest-order vector spherical functions used as discrete sources, assuring the best convergence for fibers with very large aspect ratios. The set of distributed lowest-order vector spherical functions is described by

$$\{\mathcal{M}_{mn}^{1,3}, \mathcal{N}_{mn}^{1,3}\}_{m \in \mathbb{Z}, n=1,2,\dots},$$

with

$$\begin{aligned} \mathcal{M}_{mn}^{1,3}(\mathbf{x}) &= \mathcal{M}_{m,|m|+l}^{1,3}(\mathbf{x} - z_n \mathbf{e}_3), \\ \mathcal{N}_{mn}^{1,3}(\mathbf{x}) &= \mathcal{N}_{m,|m|+l}^{1,3}(\mathbf{x} - z_n \mathbf{e}_3), \end{aligned} \quad (38)$$

where (z_n) is a bounded sequence on a segment of the z -axis.

Essentially the null-field method with discrete sources consists in the projection relations

$$\begin{aligned} \int_S \left[(\mathbf{e} - \mathbf{e}_0) \cdot \mathcal{M}_{-mn}^3 + j \sqrt{\frac{\mu_s}{\epsilon_s}} (\mathbf{h} - \mathbf{h}_0) \cdot \mathcal{N}_{-mn}^3 \right] dS &= 0, \\ \int_S \left[(\mathbf{e} - \mathbf{e}_0) \cdot \mathcal{N}_{-mn}^3 + j \sqrt{\frac{\mu_s}{\epsilon_s}} (\mathbf{h} - \mathbf{h}_0) \cdot \mathcal{M}_{-mn}^3 \right] dS &= 0, \end{aligned} \quad (39)$$

with $m = -m_{\max}, \dots, m_{\max}$, $n = 1, \dots, n_{\max}$.

The surface current densities are approximated by fields of discrete sources. There is a sequence $\{a_{mn}, b_{mn}\}$ such that

$$\begin{pmatrix} \mathbf{e} \\ \mathbf{h} \end{pmatrix} = \sum_{m=-m_{\max}}^{m_{\max}} \sum_{n=1}^{n_{\max}} a_{mn} \begin{pmatrix} \mathbf{n} \times \mathcal{M}_{mn}^1 \\ -j \sqrt{\frac{\epsilon_i}{\mu_i}} \mathbf{n} \times \mathcal{N}_{mn}^1 \end{pmatrix} + b_{mn} \begin{pmatrix} \mathbf{n} \times \mathcal{N}_{mn}^1 \\ -j \sqrt{\frac{\epsilon_i}{\mu_i}} \mathbf{n} \times \mathcal{M}_{mn}^1 \end{pmatrix}. \quad (40)$$

In the above formulation the approximated surface current densities and the null-field condition are expressed in terms of distributed lowest-order spherical vector wave functions.

Consequently, the matrix system includes Hankel functions of low orders, that generate a better conditioned system of equations compared to that obtained in the single spherical coordinate-base null-field method. The use of the lowest-order spherical multipoles is most effective for axisymmetric particles. By using a system of lowest-order spherical vector wave functions distributed along the axis of revolution, it is possible to reduce the original problem to a sequence of subproblems for each azimuthal mode.

Once the surface current densities \mathbf{e} and \mathbf{h} are determined, the scattered field outside the circumscribing sphere is obtained by using the representation theorem, as a series of radiating spherical vector wave functions

$$\mathbf{E}_s = \sum_{\nu=1}^{\infty} f_{\nu} \mathbf{M}_{\nu}^3 + g_{\nu} \mathbf{N}_{\nu}^3, \quad (41)$$

with expansion coefficients

$$\begin{aligned} f_{\nu} &= \frac{jk_s^2}{\pi} \int_S \left[\mathbf{e} \cdot \mathbf{N}_{\bar{\nu}}^1 + j \sqrt{\frac{\mu_s}{\omega_s}} \mathbf{h} \cdot \mathbf{M}_{\bar{\nu}}^1 \right] dS, \\ g_{\nu} &= \frac{jk_s^2}{\pi} \int_S \left[\mathbf{e} \cdot \mathbf{M}_{\bar{\nu}}^1 + j \sqrt{\frac{\mu_s}{\omega_s}} \mathbf{h} \cdot \mathbf{N}_{\bar{\nu}}^1 \right] dS, \end{aligned} \quad (42)$$

where $\nu = (m, n)$ and $\bar{\nu} = (-m, n)$.

Now, to derive the \mathbf{T} -matrix [37], let us assume that the incident field can be expressed inside a bounded domain containing S as a series of vector spherical wave functions

$$\begin{aligned} \mathbf{E}_0 &= \sum_{\nu=1}^{\infty} a_{\nu}^0 \mathbf{M}_{\nu}^1 + b_{\nu}^0 \mathbf{N}_{\nu}^1, \\ \mathbf{H}_0 &= -j \sum_{\nu=1}^{\infty} a_{\nu}^0 \mathbf{N}_{\nu}^1 + b_{\nu}^0 \mathbf{M}_{\nu}^1. \end{aligned} \quad (43)$$

Then, the relation between the scattered and the incident field coefficients is linear and is given by a transition matrix \mathbf{T} as follows

$$\begin{bmatrix} f_{\nu} \\ g_{\nu} \end{bmatrix} = \mathbf{T} \begin{bmatrix} a_{\nu}^0 \\ b_{\nu}^0 \end{bmatrix}. \quad (44)$$

Here,

$$\mathbf{T} = \mathbf{B} \mathbf{A}^{-1} \mathbf{A}_0, \quad (45)$$

where \mathbf{A} , \mathbf{B} and \mathbf{A}_0 are block matrices written in general as

$$\mathbf{X} = \begin{bmatrix} X_{\nu\mu}^{11} & X_{\nu\mu}^{12} \\ X_{\nu\mu}^{21} & X_{\nu\mu}^{22} \end{bmatrix}, \nu, \mu = 1, 2, \dots, \quad (46)$$

with \mathbf{X} standing for \mathbf{A} , \mathbf{B} and \mathbf{A}_0 . The elements of the matrices \mathbf{A} , \mathbf{B} and \mathbf{A}_0 are given both in [24].

The elements of the matrix \mathbf{T} are independent of the incident and scattered fields and depend only on the shape, size parameter and refractive index of the scattering particle, as well as on its orientation with respect to the coordinate system. Consequently, the \mathbf{T} need to be computed only once and then can be used in computations for any direction of light incidence and scattering.

The formulation presented in above has been implemented in a computer program. The origin of the coordinate system \mathbf{O} is positioned in the center of the cylindrical fiber, with the z -axis corresponding to the symmetry axis of the scatterer and angle θ defined with respect to the z -axis, perpendicular to z . Every point M on the surface S is described by a vector \mathbf{r} of length r and derivative dr

$$\begin{aligned} r &= \frac{b}{\cos \theta} & dr &= \frac{b \sin \theta}{\cos^2 \theta}, & 0 < \theta < \tan^{-1} \frac{a}{b} \\ r &= \frac{a}{\sin \theta} & dr &= \frac{-a \cos \theta}{\sin^2 \theta}, & \tan^{-1} \frac{a}{b} < \theta < \tan^{-1} \frac{-a}{b} \\ r &= \frac{-b}{\cos \theta} & dr &= \frac{-b \sin \theta}{\cos^2 \theta}, & \tan^{-1} \frac{-a}{b} < \theta < \pi \end{aligned} \quad (47)$$

for the straight cut end cylinder, and

$$\begin{aligned} r &= b \cos \theta + \sqrt{a^2 - b^2 \sin^2 \theta} & dr &= -b \sin \theta - \frac{b^2 \cos \theta \sin \theta}{\sqrt{a^2 - b^2 \sin^2 \theta}}, & 0 < \theta < \tan^{-1} \frac{a}{b} \\ r &= \frac{a}{\sin \theta} & dr &= \frac{-a \cos \theta}{\sin^2 \theta}, & \tan^{-1} \frac{a}{b} < \theta < \tan^{-1} \frac{-a}{b} \\ r &= -b \cos \theta + \sqrt{a^2 - b^2 \sin^2 \theta} & dr &= b \sin \theta - \frac{b^2 \cos \theta \sin \theta}{\sqrt{a^2 - b^2 \sin^2 \theta}}, & \tan^{-1} \frac{-a}{b} < \theta < \pi \end{aligned} \quad (48)$$

for the rounded end cylinder. The wave number of the region D_i is $k_i = k(\epsilon_i \mu_i)^{1/2}$, while the wave number for the free space is $k_s = k(\epsilon_s \mu_s)^{1/2}$, where $k = \omega/c$.

Recently with this method the aspect ratio of 50 was achieved for cylinder $n=1.5$ under $\lambda=488\text{nm}$ for size parameter $kl = 20\pi$ [38].

4. Finite Difference Time Domain (FDTD)

There are some other effective electromagnetic modelling methods, which are nowadays used to investigate scattering from elongated objects. One of the most famous is Finite Difference Time Domain (FDTD) [39]. With the FDTD an entire volume including the scatterer is discretized. The basis element of this discretisation is the Yee

cell, which is named after K.S.Yee [40] who originally proposed this method. The Yee cell is the basis element of the interlocked grid with the electric field representing an unknown on the edges of one grid and the magnetic field the unknowns on the other, corresponding to the faces of the grid. The differential form of Maxwell's equations are solved directly. A difference approximation is applied to evaluate the space and time derivatives of the field. The fields are computed by a time marching scheme. Each grid point of the volume may have different values of permittivity so that inhomogeneous scatterer can be computed. For simulation of scattering special absorbing boundary conditions are needed that the wave is not reflected at the open boundary of the discretised volume. A near-field to far-field transformation is needed to compute the scattered far field from the near-field values of the computational volume. The FDTD method requires not only the scatterer to be discretised, but also part of the near-field around it. The grid distance must be smaller than the wavelength of the incident wave. The advantage of this method is that only nearby grid points are calculated and there is no matrix to store and invert, but care should be paid to a choice of grid step to avoid instability of results. The FDTD is often used for investigation light scattering from hexagonal ice crystals [41], which is particularly important for investigation climate effects [42], but the capability of method allows to calculate quite small aspect ratio: 6 for hexagonal ice column ($n=1.311+3.11*10^{-9}$), $\lambda=0.55\mu\text{m}$ with size parameter $2\pi a/\lambda$ up to 10 [16].

5. Discrete Dipole Approximation (DDA)

The Discrete Dipole Approximation (DDA) developed by Purcell and Pennypacker [43] is another general technique for calculating the scattering from particles of arbitrary shapes. Later this method was a subject of active research in many diverse fields, like investigation of properties of interstellar dust and ice-crystals [44], [45]. The first public Fortran code was developed by Draine [46]. In frame of DDA the solid particle is replaced by an array of number of point dipoles. The spacing between dipoles is small compared with a wavelength. The dipoles are assumed to occupy positions on a cubic lattice. Each dipole has an oscillating polarization in response to both an incident plane wave and the electric fields due to all of the other dipoles in the array. The number of dipoles depends on the required numerical accuracy, the problem geometry and the refractive index [47].

In recent research in ice particle in clouds the aspect ratio of 9 was achieved for cylinders of length till 0.002mm under a frequency range 90-900 GHz [48]. The last investigation in optical particle characterization obtain the results for particle with aspect ratio of 8, $n=1.5$, under the wavelength $\lambda=532\text{nm}$ were presented in [49].

6. Spheroidal expansion

Another method which looks very attractive is spheroidal expansion. In frame of this method the surface of the scattering spheroid coincides with one of the coordinate surfaces. The incident, transmitted and scattered fields are expanded in terms of spheroidal wavefunctions. The coefficients of the scattered field are then found by imposing the boundary conditions on the particle surface. As Maxwell's equations are separable in a spheroidal coordinate system, the separation of variables approach can be

applied. The original theory was presented in a paper by Asano and Yamamoto [50], and results for prolate spheroids for aspect ratio till 5 and particle size parameters up to 35 were given in [51]. Another approach of this method was elaborated by Voshinnikov and Farafonov for oblate and prolate spheroids [52]. Recently this approach was applied to prolate cylinders [53] and results for cylinders with aspect ratio till 100 for $n=1.5$, and size parameters up to 3 were presented. The good review of some other light scattering theories may be found in [54].

7. Computational results

To show the capabilities of the GMT methods presented above and which are used by our group we would like to present some computational results. All the presented results shows the dependence of differential scattering cross section (DSC) in μm^2 from the scattered angle θ in the azimuthal plane $\phi = 0^\circ$ which contains the symmetry axis of the fiber. The incident field is perpendicular to the fiber.

Using MMP it's possible to calculate not only axisymmetrical scatterers, but also a bent fiber. [22] Figure 1 shows the result for SiO ($n=1.67$) fiber with length $l=5\mu\text{m}$ and diameter $D=0.5\mu\text{m}$ obtained by FORTRAN program on base of MMP and the bent fiber with the same parameters, the centre of bending coincides with the direction of incident field incoming: $\theta_0 = 0^\circ$, $\lambda=0.488\mu\text{m}$. one can see that such bounding essentially change the the scattering diagramm at scattering angle of 45 degrees and higher. The main difference to the scattering diagram of a straight fibers is in the back scattering region. Thus it is that by detecting forward scattering the correct length can be measured even of a slightly bent fiber.

DSM allows to calculate scattering even from very elongated fibers [34] and for large diameters of fibers with small aspect ratios. To demonstrate the capability of the method Figure 2 shows the light scattering from elongated SiO cylinder with $l=4\mu\text{m}$, $D=0.4\mu\text{m}$ and aspect ratio 50 for P polarized incident wave. To show that scattering from

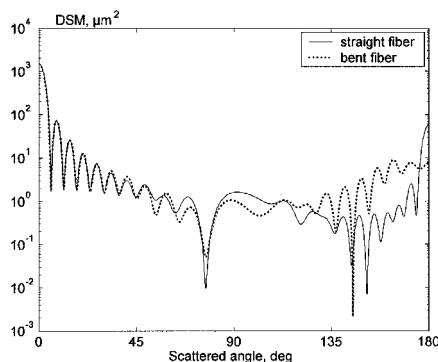


Figure 1. DSC versus scattering angle θ in the plane of incidence $\phi=0$ from SiO ($n=1.67-0.00i$) cylinder, $l=20\mu\text{m}$, $D=0.4\mu\text{m}$, (aspect ratio 50), P-polarization, incident angle $\theta_0=0^\circ$, $\lambda = 0.488\mu\text{m}$.

rather long fiber of $16\mu\text{m}$ length can be computed Figure 3 shows results for SiO_2 fiber of large diameter $D = 2\mu\text{m}$ with aspect ratio of 8.

Null-field method with discrete sources gives a possibility to calculate not only mostly used model of hemi-spherical (round) ended fiber, but also a fiber with flat ends [38]. The comparison of two glass ($n=1.5$) fibers with length $l=6\mu\text{m}$ and diameter $D=0.2\mu\text{m}$ but of different shape one can see on Figure 4. One can see that even with this aspect ratio of 30 from the scattering diagramm one can recognize fibers rounded or flat at their ends.

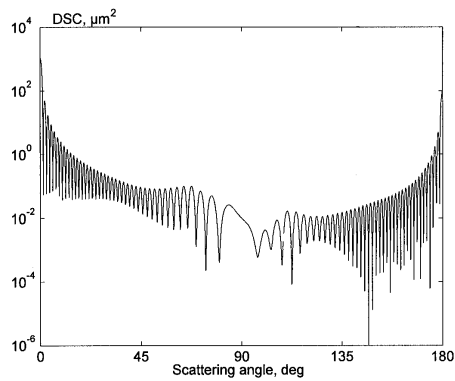


Figure 2. DSC versus scattering angle θ in the plane of incidence $\phi=0$ from SiO ($n=1.67-0.00i$) cylinder, $l=20\mu\text{m}$, $D=0.4\mu\text{m}$, (aspect ratio 50), P-polarization, incident angle $\theta_0=0^\circ$, $\lambda = 0.488\mu\text{m}$.

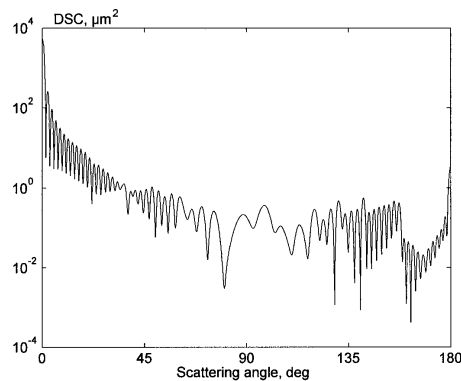


Figure 3. DSC versus scattering angle θ in the plane of incidence $\phi=0$ from SiO_2 ($n=1.46-0.00i$) cylinder, $l=16\mu\text{m}$, $D=2\mu\text{m}$, (aspect ratio 8), P-polarization, incident angle $\theta_0=0^\circ$, $\lambda = 0.488\mu\text{m}$.

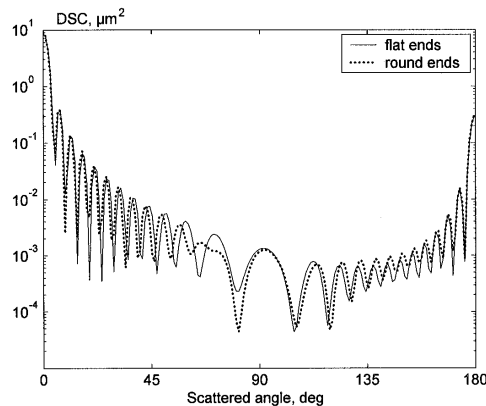


Figure 4. DSC versus scattered angle θ , in the plane of incidence $\phi=0$, for flat-end and round-end glass ($n=1.5 - 0.0i$) cylinders, $l=6\mu\text{m}$, $D=0.2\mu\text{m}$ (aspect ratio 30), P-polarization, incident angle $\theta_0=0$, $\lambda=0.628\mu\text{m}$.

8. Conclusion

In this paper we reviewed progress in simulation of light and electromagnetic scattering by elongated objects. To summarise, it has been found that volume discretisation methods like FDTD, DDA are quite versatile but because of high computational demand restricted to show scatterers (composed to the incident wavelength). They have mainly been applied to scattering by cirrus ice particles. Surface based methods need much less computer power. The standard **T**-matrix method is the most well known, but restricted to objects having an aspect ratio of about 20. With the Generalized Multipole methods there has been the most progress in recent years. With the DSM scattering by rotationally symmetric cylinders having an aspect ratio of 100 can be computed. Computer demand is quite low with this method. The same is true for the Null Field Method with Discrete Sources. Aspect ratio of 50 for a rotationally symmetric objects can be achieved. The advantage of this method is that the **T**-matrix can be computed which is thus available for post-processing, such as orientation averaging. The MMP is there for some years but for the first time scattering by long cylinders have been demonstrated. In the examples presented in paper the aspect ratio used is 10 but the higher value should easily be achievable. As this method is not restricted to axisymmetric scatterers scattering results for bent cylindrical fibers have been presented for the first time.

We hope that with this review the reader will be able to consider different methods for his specific light scattering problem.

Acknowledgement 1

We would like to acknowledge Sorin Pulbere and Roman Schuh for contributing to this review.

Acknowledgement 2

We gratefully acknowledge support of this work by Deutsche Forschungsgemeinschaft (DFG).

References

1. Liou, K.N. 1986, *Mon. Weather Rev.*, 114, 1167.
2. Stephens, G.L., Tsay S.C., Stackhouse, P.W., Flatau P.J. 1990, *J. Atmos. Sci.*, 47, 1742.
3. Green, E., Gustafson, Bo A.S., Dermott, S., Fechtig, H., 2001, *Interplanetary Dust*, Springer, Berlin.
4. Videen, G., Kocifaj, M., 2002, *Optics of Cosmic Dust*, Kluwer Academic Publishers, Netherlands.
5. Kommission Reinhaltung der Luft: Sicherer Umgang mit Fasermaterialien, 1998, VDI Berichte 1417, VDI Verlag GmbH, Düsseldorf.
6. Höfert, N., Lehmann, C., Sharafi, M., 1999, *Gefahrstoffe - Reinhalt. Luft* 59, 193.
7. Bauckhage, K., Bottlinger, M., Ebert, F., Fissan, H., Rippenberger, S., Sommer, K., Weichert, R., Wriedt, T. in *Kommission Reinhaltung der Luft im VDI und DIN: Sicherer Umgang mit Fasermaterialien*, 1998, VDI-Berichte 1417, VDI Verlag, Düsseldorf, 2513.
8. Waterman, P.C., 1965, *Proc. IEEE* 53, 805.
9. Waterman, P.C., 1969, *Alta Frequenza (Speziale)* 38, 349.
10. Waterman, P.C., 1971, *Phys. Rev. D* 3, 825.

11. Mishchenko, M.I., Travis, L.D., Mackowski, D.W., 1996, *J. Quant. Spectrosc. Radiat. Transfer.*, 55, No.5, 535.
12. Zakharova, N.T., Mishchenko, M.I., 2000, *Applied Optics.* 39, No. 27, 5052.
13. Havemann, S., Baran, A.J., 2001, *JQSRT* 70, 139.
14. Havemann, S., Baran, A.J., Edwards, J.M., 2003, *JQSRT* special issue in press.
15. Zakharova, N.T., Mishchenko, M.I., 2001, *JQSRT* 70, 465.
16. Mishchenko, M.I., Hovenier, J.W., Travis, L.D., 2000, *Light Scattering by Nonspherical Particles: Theory, Measurements and Applications*, Academic Press, San Diego.
17. Wriedt, T., 1999, *Generalizes Multipole Techniques for Electromagnetic and Light Scattering*. Elsevier Science. Amsterdam.
18. Ludwig, A.C., 1991, *Comp. Phys. Commun.* 68, 306.
19. Al-Rizzo, H.M., Tranquilla, J.M., 1995, *Applied Optics.*, 34, No.18, 3502.
20. Hafner, C., Bomholt, K. 1993, *The 3D electrodynamic wave simulator*, Wiley, Chichester.
21. Sagehorn, H., List, J., Wiegand, T., Weichert, R., Wriedt, T., 2001, *Part. Part. Syst. Char.* 18 No.2, 55.
22. Schuh, R., Wriedt, T., 2003, *Light scattering by bent cylindrical fibers for fiber length and diameter characterization*, *Part. Part. Syst. Char.*, submitted.
23. Wriedt, T., Doicu, A., Comberg, U., Sagehorn, H., Schuh, R., 2000, in G. Gousbet (editor) *Scattering of shaped light beams and applications*, Research Signpost, Trivandrum, India.
24. Doicu, A., Eremin, Y., Wriedt, T., 2000, *Acoustic and Electromagnetic Scattering Analysis using Discrete Sources*, Academic Press, London.
25. Kupradze, V.D., 1967, *Usp. Mat. Nauk.* 22, No.2, 58.
26. Okuno, Y., Ikuno, H., 1992, *Radiotekh. Electron. (Moscow).* 37, No.10, 1744.
27. Sveshnikov, A.G., Eremin, Yu.A., 1980, *Izv. Vyssh. Uchebn. Zaved. Radiofiz.* 23, No.8, 580.
28. Eremin, Y., 2000, *J. Commun. Techn. Electron.* 45, 269.
29. Eremina, E.Yu., Sveshnikov, A.G., 1998, *J. Appl. Electromagnetism.* 1, No3, 25.
30. Eremin, Y., Wriedt, T., 2002, *Optics Communications.*, 214, 39.
31. Colton, D., Kress, R., 1992, *Inverse acoustic and electromagnetic scattering theory*, Springer, Berlin.
32. Eremin, Y., Orlov, N., Sveshnikov, A., 1999, in *Generalizes Multipole Techniques for Electromagnetic and Light Scattering*, edited by Wriedt, T., Elsevier Science, Amsterdam, 39.
33. Voevodyn, V., Kuznetsov, A., 1982, *Matrices and calculations*, Science, Moscow.
34. Eremina, E., Eremin, Y., Wriedt, T., 2003, *Journal of Modern Optics*, submitted.
35. Doicu, A., Wriedt, T., 1997, *Optics Communications* 139, 85.
36. Doicu, A., Wriedt, T., 2001, *JQSRT* 70, 663.
37. Doicu, A., Wriedt, T., 1999, *J. Opt. Soc. Am. A.* 16, 2539.
38. Pulbere, S., Wriedt, T., 2003, *Part. Part. Syst. Charact.*, submitted.
39. Taflove, A., 1995, *Computational electrodynamics: the finite difference time-domain method*, Artech House, Boston.
40. Yee, K.S., 1966, *Antennas Propag.*, 14, 302.
41. Yang, P., Liou, K.N., 1996, *J. Opt. Soc. Am. A.* 13, 2072.
42. Yang, P., Liou, K.N., 1995, *J. Opt. Soc. Am. A.* 12, No.1, 162.
43. Purcell, E.M. Pennypacker, C.R., 1973, *Astrophys. J.* 186, 705.
44. Draine, B.T., 1988, *Astrophys. J.* 333, 848.
45. Flatau, P.J., Stephens, G.L., Draine, B.T., in *International radiation symposium*, Lenoble, J. and Geleyn J.-F. editors, A. Deepak Publishing, Hampton, Virginia, USA, 72, Lille, France.
46. Draine, B.T., Flatau, P.J., *DDSCAT*. *JQSRT* 44, I. Software package *JQSRT-020-S90*.
47. Draine, B.T., Flatau, P.J., 1994, *J. Opt. Soc. Am. A* 11, 1491.
48. Miao, J., Buehler, S., Kunzi, K., 9-14 July 2001, 16 ARSS 2001, Sydney, Australia.
49. Sachweh, B., Barthel, H., Polke, R., Umhauer, H., Buettner, H., 1999, *J. Aerosol Sci.* 30, N10, 1257.

-
50. Asano, S., Yamamoto, G., 1975, *Appl. Opt.* 14, 29.
 51. Asano, S., 1979, *Appl. Opt.* 18, 712.
 52. Voshinnikov, N.V., Farafonov, V.G., 1993, *Astrophys. Space Sci.* 204, 19.
 53. Voshinnikov, N.V., Farafonov, V.G., 2002, *Meas. Sci. Technol.* 13, 249.
 54. Wriedt, T., 1998, *Part. Part. Syst. Character.* 15, 67.